ISSN (Print) 1226-1750
ISSN (Online) 2233-6656
Journal of Magnetics 18(4), 380-385 (2013) http://dx.doi.org/10.4283/JMAG.2013.18.4.380

Metastable Vortex State of Perpendicular Magnetic Anisotropy Free Layer in Spin Transfer Torque Magnetic Tunneling Junctions

Chun-Yeol You[1] and Hyungsuk Kim[2]*

[1]*Department of Physics, Inha University, Incheon 402-751, Korea*
[2]*Department of Electrical Engineering, Kwangwoon University, Seoul 139-701, Korea*

(Received 30 September 2013, Received in final form 8 October 2013, Accepted 11 October 2013)

We find a metastable vortex state of the perpendicular magnetic anisotropy free layer in spin transfer torque magnetic tunneling junctions by using micromagnetic simulations. The metastable vortex state does not exist in a single layer, and it is only found in the trilayer structure with the perpendicular magnetic anisotropy polarizer layer. It is revealed that the physical origin is the non-uniform stray field from the polarizer layer.

Keywords : magnetic random access memory (MRAM), micromagnetic simulation, perpendicular magnetic anisotropy, vortex, spin transfer torque

1. Introductions

Generally, a vortex configuration is an energetically stable state with specific conditions in the nanoscale structures [1-3]. In certain sizes of nanostructures, a single domain state is not energetically favorable due to the strong demagnetization energy. Therefore, the vortex state is formed by reducing the demagnetization energy by increasing the exchange coupling energy for in-plane magnetic materials. There are many researches on the vortex dynamics with the ac- and dc- external fields and spin polarizing currents [4-7] as well as with the devices [8, 9]. However, all researches regarding the vortex states are considered only in the in-plane magnetic anisotropy (IMA) materials.

There is no known stable vortex state in the perpendicular magnetic anisotropy (PMA) materials so far within our best knowledge. In this study, we present a metastable vortex state for PMA materials in a nano-disk structure for the spin transfer torque magnetic random access memory (STT-MRAM). Because the STT-MRAM requires a PMA free layer in order to overcome the thermal stability problems [10, 11], researches about the PMA free layer are timely important. In the present work, we investigate the stable state of the free layer of the typical circular magnetic tunneling junctions (MTJ) and a single layer structure by employing micromagnetic simulations based on Object-Oriented MicroMagnetic Framework (OOMMF) [12] using the public STT extension module [13]. We discovered that the metastable vortex state can be formed in the MTJ with the polarizer layers; however, such vortex states are not found in the single nano-disks. The PMA vortex state is formed by balancing between demagnetization energy, uniaxial perpendicular magnetic anisotropy energy, exchange coupling energy and the Zeeman energy due the stray field from the polarizer layer. Therefore, it is much more complex than the IMA vortex state and further, it is not easy to analyze analytically. However, it is clear that that the non-uniform stray field from the polarizer layer plays a crucial role in the formation of the vortex state.

2. Micromagnetic Simulations

Figure 1 shows the typical PMA MTJ structures and a single PMA free layer. F_{Free}, Insulator and $F_{Polarizer}$ layers stand for the free, insulator and polarizer layer. The thickness of the F_{Free}, Insulator and $F_{Polarizer}$ layers are 2, 1 and 1 nm, respectively. The saturation magnetizations of F_{Free} and $F_{Polarizer}$ are 1.3×10^6 A/m, and the interface PMA energy and K_s of the polarizer layers are fixed to 2.6×10^{-3} J/m^2 without volume anisotropy energy. The surface PMA of the free layer are varied from 0.5×10^{-4} to 1.0×10^{-3} J/m^2. In the micromagnetic simulations, we set the perpendicular volume anisotropy K_u with the relation of $K_u = K_s/$

©The Korean Magnetics Society. All rights reserved.
*Corresponding author: Tel: +82-2-940-8373
Fax: +82-2-940-5141, e-mail: hskim@kw.ac.kr

© 2013 Journal of Magnetics

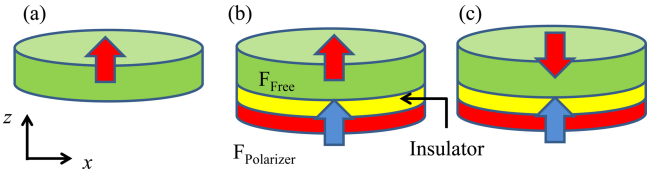

Fig. 1. (Color online) The schematic structures of (a) single layer, (b) parallel state of MTJ, and (c) anti-parallel state of MTJ with the coordinate systems.

t_{Free} (= 1.0 × 10^5 to 2.0 × 10^6 J/m^3 for 2 nm t_{Free}) in order to implement the interface anisotropy. The shapes of the MTJ are fixed with the 40-nm diameter circular disk, as shown in Fig. 1. The exchange stiffness constant A_{ex} = 3.0 × 10^{-11} J/m and Gilbert damping constant α = 0.02 are fixed in the present work. The unit cell size of 1 × 1 × 1 nm^3 are used. More details of the micromagnetic simulations can be found in our previous report [13]. For simplicity, we performed all simulations at 0 K.

3. Stable States of the Single Free Layer

In order to find the stable state of a single layer, we set the whole magnetization directions of the single layer to +z direction, and relaxed them. Due to the finite size edge effect, the spins at the edge are slightly deviated from the +z-axis, when the K_u is large. We varied K_u from 1.0 × 10^5 to 2.0 × 10^6 J/m^3, and found the stable states. In Figs. 2(a)-(c), we depicted the snapshots of the selected cases. For the smallest K_u of 1.0 × 10^5 J/m^3, the stable state is an in-plane single domain, as shown in Fig. 2(a). When we set K_u = 8.0 × 10^5 J/m^3, the stable state is also a single domain (Fig. 2(b)); however, there are finite out-of-plane components. In our snapshot, the red color indicates +z components. The directions of the in-plane component are not meaningful, because there is no in-plane anisotropy in our problems. When we increase K_u to 10.0 × 10^5 J/m^3, the stable state is now out-of-plane, as shown in Fig. 2(c). More details of the stable state dependence on K_u will be discussed later (see Fig. 8).

In a simple single domain model for an infinite film, the system energy density is given by

$$E_T = -K_u \cos^2\theta + 1/2\mu_0 M_s^2 \cos^2\theta$$
$$= (-K_u + 1/2\mu_0 M_s^2)\cos^2\theta \quad (1)$$

Here, θ is an angle of the magnetization from +z-axis. The energy equation turns out to a kind of uniaxial anisotropy equation. The competition between PMA energy and the demagnetization energy determine the stable state. Therefore, when $K_u > 1/2\mu_0 M_s^2$, the out-of-plane configuration is stable, whereas when $K_u < 1/2\mu_0 M_s^2$, the in-plane configuration is stable. However, we examined the finite nano-disks, such that the simple single model is not correct. It must be noted that the oblique state, such as Fig. 2(b) (K_u = 8.0 × 10^5 J/m^3), cannot exist according to Eq. (1); however, such oblique state is energetically stable, as indicated in Fig. 3. We plot the total system energy as a function of time for the single layers in Fig. 3. The difference of the total energy ΔE_T between K_u = 10^5 and 10^6 J/

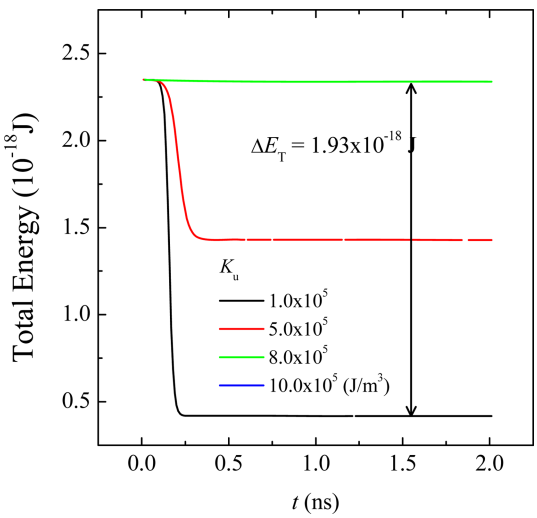

Fig. 3. (Color online) Time dependent total energy for the single layer for various K_u (1.0, 5.0, 8.0, 10.0 × 10^5 J/m^3).

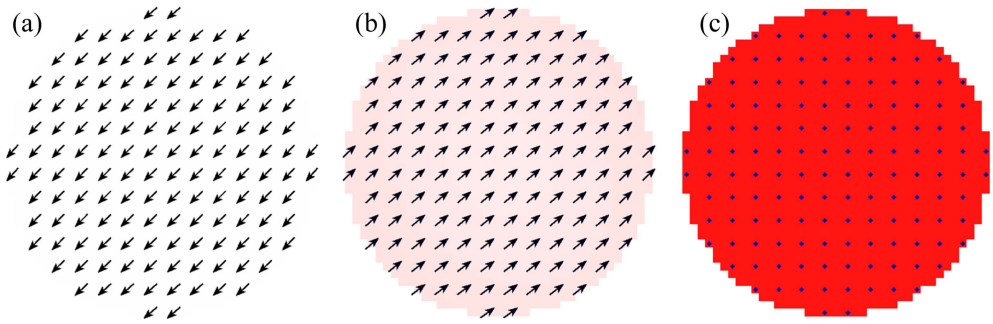

Fig. 2. (Color online) Snapshots of the single layers for K_u of (a) 1.0, (b) 8.0, and (c) 10.0 × 10^5 J/m^3.

m^3 is 1.93×10^{-18} J, corresponding to 7.68×10^5 J/m^3 for the 40-nm diameter and 2-nm thick nano-disk, as indicated by the vertical arrow. Based on Eq. (1), the ΔE_T is $\Delta E_T = E_T(K_u = 10^6, \theta = \pi/2) - E_T(K_u = 10^5, \theta = 0) = -10^5 + 1.06 \times 10^6$ J/m^3 ~ 9×10^5 J/m^3. The discrepancy between the single domain model and micromagnetic simulation results is clear. The demagnetization energy in Eq. (1) is for the infinite plane, not for the finite nano-disk; hence, the real demagnetization energy is smaller than $1/2\mu_0 M_s^2$. We can conclude that the 40-nm diameter nano-disk is small enough to form a single domain for the single layer.

4. Stable States of the MTJ nano-disk

Figures 4(a)-(c) show the stable states of the free layers of MTJ for various K_u. Initially, we set all magnetization of the MTJ perpendicular to the plane (+z-direction, parallel (P)-state), and relax them for 5 ns. For K_u of 10^6 J/m^3, the stable state is a perpendicular magnetization configuration and is parallel to the polarizer layer, as presented in Fig. 4(c). The polarizer layer magnetizations are always parallel to the +z-axis (not shown here), and the stray field is also a +z-axis. However, when we set K_u = 1 and 5×10^5 J/m^3, the stable states are different from the single layer cases due to the stray field from the polarizer layer. As shown in Figs. 4(a) and (b), the stable state is a kind of a vortex state, in spite of the PMA, and is sufficiently small-sized with regard to the nano-disk. For the single layer, the stable state is a single domain with in-plane magnetization, as shown in the previous section. However, a stable vortex state is formed in the MTJ structure. It implies that the dipole interaction

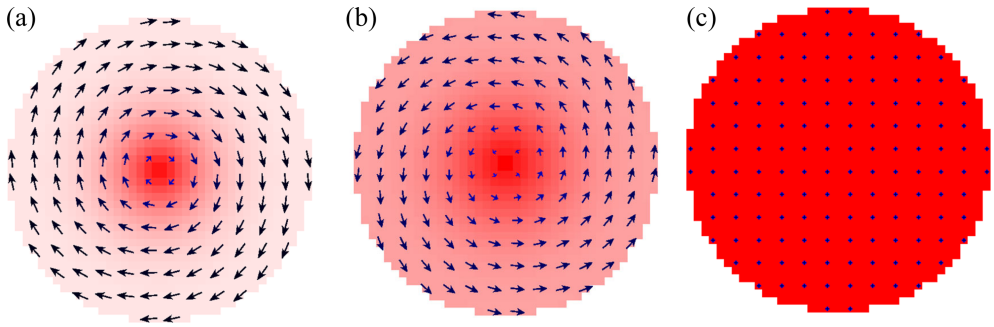

Fig. 4. (Color online) Snapshots of the free layer for the initially P-state MTJ structure with various K_u of (a) 1.0, (b) 5.0, and (c) 10.0×10^5 J/m^3.

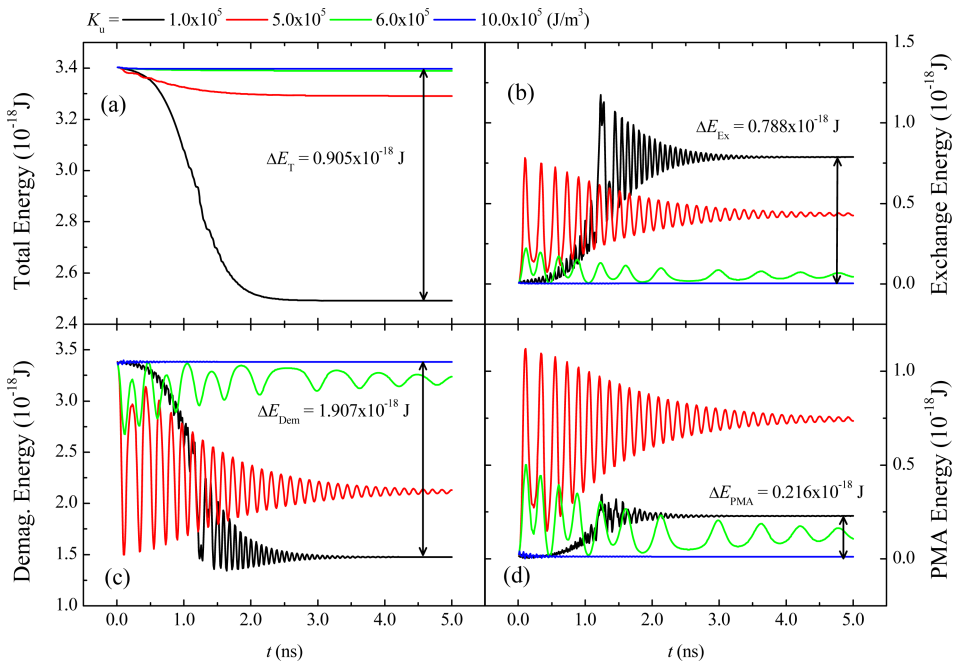

Fig. 5. (Color online) Time dependent (a) total, (b) exchange, (c) demagnetization, and (d) the PMA energies for the initially P-state MTJ structure with various K_u (1.0, 5.0, 6.0, 10.0×10^5 J/m^3).

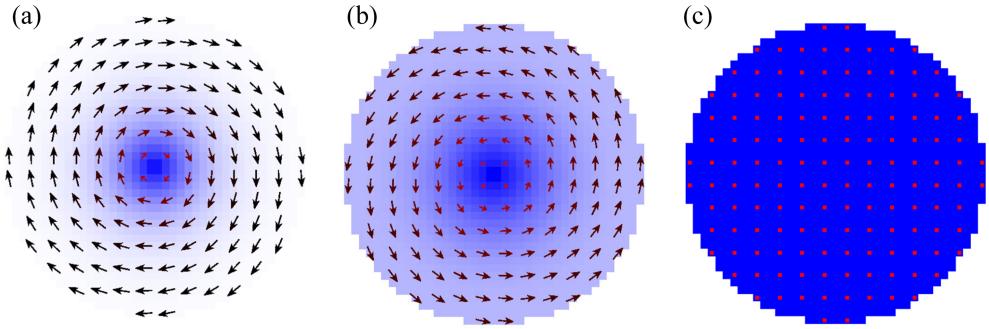

Fig. 6. (Color online) Snapshots of the free layer for the initially AP-state MTJ structure with various K_u of (a) 1.0, (b) 6.0, and (c) 10.0×10^5 J/m^3.

between the polarizer and free layers plays essential roles in the formation of the stable state. Similar to the vortex for the in-plane anisotropy materials, the PMA vortex has a vortex core, where the magnetization direction is perpendicular to the plane, and other parts are in-plane magnetization with a chiral structure. Here, the chirality of the vortex can be either clockwise or counter-clockwise, and the energies of the clockwise or counter-clockwise states are the same. Therefore, the chirality will be determined by the initial conditions. Figures 5(a)-(d) show the time dependent total, exchange, demagnetization and PMA energies for the selected K_u. The vertical arrows are the energy difference between K_u of 10^5 and 10^6 J/m^3. It is clear that the total energy of $K_u = 10^5$ J/m^3 is much lower than 10^6 J/m^3, as shown in Fig. 5(a). However, Fig. 5(b) shows that the exchange energies of the vortex states are larger than a single domain state, and Fig. 5(c) shows that the demagnetization energies of the perpendicular state are larger than the vortex state case. The PMA energies of the vortex states are larger than the perpendicular state, as shown in Fig. 5(d). It is clear that the demagnetization energy can be lowered by forming the vortex state, despite it costs of the exchange and PMA energies. Here, the vortex core points the +z-direction is the initial direction of the free layer.

We conducted the same simulations for the initially anti-parallel (AP) state, where the magnetizations of the free layer are set to the –z-direction. We obtained similar vortex states, as shown in Figs. 6(a)-(c), depending on the K_u values. It must be noted that the magnetization direc-

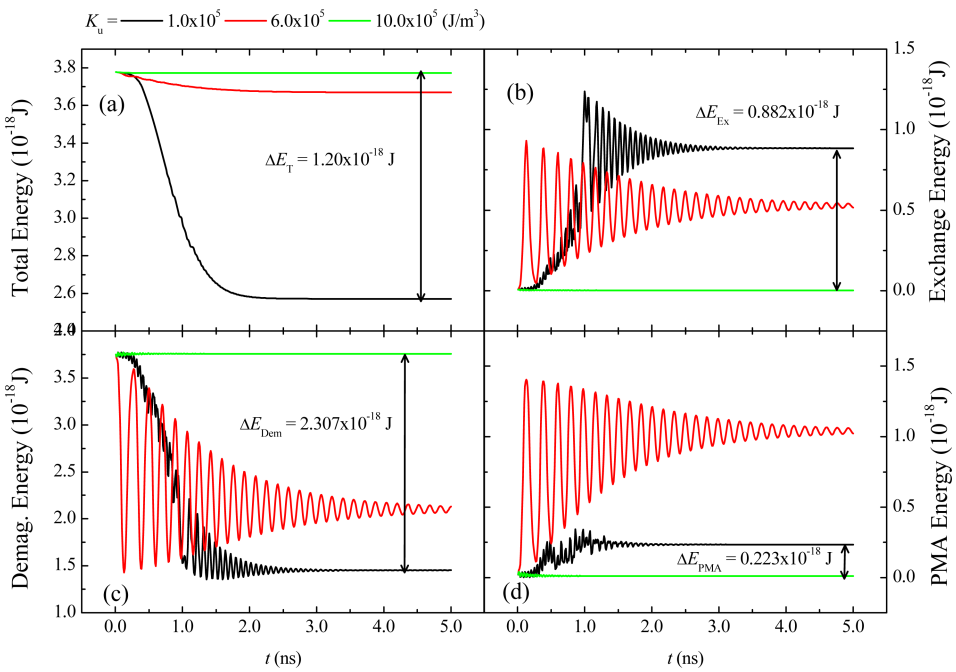

Fig. 7. (Color online) Time dependent (a) total, (b) exchange, (c) demagnetization, and (d) the PMA energies for the initially AP-state the MTJ structure with various K_u (1.0, 6.0, 10.0×10^5 J/m^3).

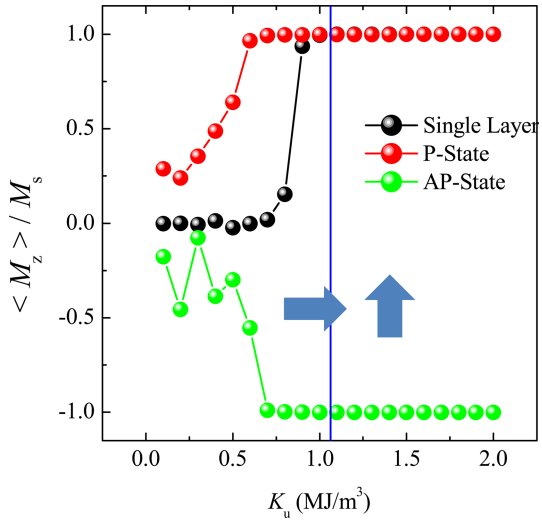

Fig. 8. (Color online) Stable average normalized out-of-plane magnetizations $\langle M_z \rangle / M_s$ with the various K_u for the single layers, initially P-states and initially AP-states. The ground state of the left (right) hand side of the vertical line is an in-plane (out-of-plane) magnetization configuration for the infinite films.

tion of the vortex core are –z-direction, same as the initial direction; however, it is anti-parallel to the stray field from the polarizer layer. We plotted the total, exchange, demagnetization and PMA energies for the AP-state in Figs. 7(a)-(d). If we compare the P- and AP-states, the main energy difference is demagnetization energy. Because the AP-state is energetically unfavorable for the dipole interaction, the demagnetization energy of the P-state is lower than AP-state's for $K_u = 10^6$ J/m^3, as shown in Fig. 5(c) and 7(c). However, the demagnetization energy of the vortex states ($K_u = 10^5$ J/m^3) of P- and AP-state are almost the same, as demonstrated in Fig. 5(c) and 7(c). Because the magnetizations of the vortex state are almost in-plane, except for the small core part, the difference of the demagnetization energies P- and AP-state must be small.

We plot the average normalized out-of-plane magnetization $\langle M_z \rangle / M_s$ for various K_u in Fig. 8 for the single, P- and AP-state. The vertical line is an anisotropy energy, where the easy axis is changed, $K_u > 1/2\mu_0 M_s^2$, for the infinite plane. For a large enough K_u, the P- and AP-state are stable. When the K_u decreases, $\langle M_z \rangle / M_s$ of the single layer goes to zero, which implies that there is no out-of-plane component, purely an in-plane magnetization. However, the MTJ structure, $\langle M_z \rangle / M_s$ has non-zero values, implying that the the vortex states are formed for small K_u. It must be noted that the signs of $\langle M_z \rangle / M_s$ are the same as the initial conditions.

Before the conclusion, we must discuss about the thermal energy contribution. Due to the fact that the micromagnetic simulation does not consider thermal energy, thermal agitation will destroy the vortex state. However, the energy difference between P- or AP-state to the vortex state is an order of 10^{-18} J, which is much larger than the typical thermal energy $k_B T \sim 4.14 \times 10^{-21}$ J for room temperature.

5. Conclusions

Many studies on PMA free layers to find optimal conditions for the STT-MRAM applications [14, 15]. However, with our best knowledge, possible metastable vortex state is never predicted or observed in the PMA nano-disk. The predicted nano vortex structure has different magnetic characteristics from the in-plane vortex structure due to the small size. It will open new spin dynamics with different characteristic frequencies and so on. Since the finding vortex state can be exist in real devices, more detail study about PMA vortex state must be addressed.

Acknowledgements

This work has been supported by the Research Grant of Kwangwoon University.

References

[1] T. Shinjo, T. Okuno, R. Hassdorf, K. Shigeto, and T. Ono, Science **289**, 930 (2000).
[2] K. Yu. Guslienko, V. Novosad, Y. Otani, H. Shima, and K. Fukamichi, Phys. Rev. B **65**, 024414 (2001).
[3] K. Yu. Guslienko, B. A. Ivanov, V. Novosad, Y. Otani, H. Shima, and K. Fukamichi, J. Appl. Phys. **91**, 8037 (2002).
[4] J.-S. Kim, M. Kläui, M. V. Fistul, J. Yoon, C.-Y. You, R. Mattheis, C. Ulysse, and G. Faini, Phys. Rev. B **88**, 064402 (2013).
[5] J.-S. Kim, O. Boulle, S. Verstoep, L. Heyne, J. Rhensius, M. Kläui, L. J. Heyderman, F. Kronast, R. Mattheis, C. Ulysse, and G. Faini, Phys. Rev. B **82**, 104427 (2010).
[6] S. Kasai, Y. Nakatani, K. Kobayashi, H. Kohno, and T. Ono, Phys. Rev. Lett. **97**, 107204 (2006).
[7] Jun-Yeon Kim and Sug-Bong Choe, J. Magnetics **12**, 113 (2007).
[8] Ki-Suk Lee, Dong-Soo Han, and Sang-Koog Kim, Phys. Rev. Lett. **102**, 127202 (2009).
[9] Sang-Koog Kim, Ki-Suk Lee, and Dong-Soo Han, Appl. Phys. Lett. **95**, 082507 (2009).
[10] S. Ikeda, J. Hayakawa, Y. M. Lee, F. Matsukura, Y. Ohno, T. Hanyy, and H. Ohno, IEEE Trans. Elec. Dev. **54**, 991 (2010).
[11] S. Ikeda, M. Miura, H. Yamanoto, K. Mizunuma, H. D. Gan, M. Endo, S. Kanai, J. Hayakawa, F. Matsukura, and H. Ohno, Nat. Mat. **9**, 721 (2010).

[12] M. J. Donahue and D. G. Porter: OOMMF User's Guide, Ver. 1.0, Interagency Report NISTIR 6376, NIST, USA (1999).
[13] C.-Y. You, J. Magnetics **17**, 73 (2012).
[14] E. H. M. van der Heijden, K. J. Lee, Y. H. Choi, T. W. Kim, H. J. M. Swagten, C.-Y. You, and M. H. Jung, Appl. Phys. Lett. **102**, 102410 (2013).
[15] Jungbum Yoon, Sol Jung, Youngha Choi, Jaehun Cho, Chun-Yeol You, Myung-Hwa Jung, and H. I. Yim, J. Appl. Phys. **133**, 17A342 (2013).